Molecular Crystals and Liquid Crystals

Publication details, including instructions for authors and subscription information:
http://www.tandfonline.com/loi/gmcl20

Role of Microscopic Defects in the Plasticity of Lamellar Materials

C. Blanc [a] , N. Zuodar [b] , J.-L. Martin [b] , I. Lelidis [c] & M. Kleman [d]

[a] GDPC, UMR 5581, Univ. MontpellierII, Montpellier Cedex 5, France

[b] Département de Physique EPFL, Lausanne, Switzerland

[c] LPMC, Université de Picardie, Amiens, France

[d] LMCP, UMR 7590, Paris Cedex 05, France

Version of record first published: 18 Oct 2010

To cite this article: C. Blanc, N. Zuodar, J.-L. Martin, I. Lelidis & M. Kleman (2004): Role of Microscopic Defects in the Plasticity of Lamellar Materials, Molecular Crystals and Liquid Crystals, 412:1, 85-92

To link to this article: http://dx.doi.org/10.1080/15421400490431903

Mol. Cryst. Liq. Cryst., Vol. 412, pp. 85/[1695]–92/[1702], 2004

ISSN: 1542-1406 print/1563-5287 online
DOI: 10.1080/15421400490431903

ROLE OF MICROSCOPIC DEFECTS IN THE PLASTICITY OF LAMELLAR MATERIALS

*C. Blanc**
GDPC, UMR 5581, Univ. MontpellierII, F-34095 Montpellier Cedex 5, France

N. Zuodar and J.-L. Martin
Département de Physique EPFL, CH-1015 Lausanne, Switzerland

I. Lelidis
LPMC, Université de Picardie, 80039 Amiens, France

M. Kleman
LMCP, UMR 7590, T16 case 115, 4 place Jussieu, F-75252 Paris Cedex 05, France

The behavior of lamellar materials under strain is not yet completely understood, either for large shears where macroscopic defects (onions, focal conic domains) are formed, or even in small-strains experiments where the deformation is ruled by dislocations.

We have developed a micro-plasticity experiment, in which we impose a controlled strain to an homeotropic smectic A sample and observe, under microscope, the associated motion of edge dislocations (a dynamical extension of the well-known experiment [1] at rest described in R. B. Meyer et al., Phys. Rev. Lett. 41, 1393 (1978)). We note that edge dislocations are strongly pinned by screw dislocations. We explain how this pinning is at the origin of a yield strain. We furthermore study the dynamics of climbing edge dislocations and evidence a morphological transition from a jerky motion to a viscous regime. We clarify the role of the pinning in this transition.

Keywords: edge and screw dislocations; plasticity; smectic liquid crystal

A number of investigations, led over many years [2–8], all indicate that defects, *viz.* focal conic domains, screw and edge dislocations, play an important role in the plastic behaviour of smectics under shear. Although

*Corresponding author. E-mail: blanc@gdpc.univ-montp2.fr

some of the mechanisms in play have already been tentatively described [3,7], the situation is far from being satisfactory, because of a lack of in-situ observations. In this work, we bring some new elements to the question of the interactions between dislocations at a microscopic level. A much more detailed report, with quantitative data and microscopic models of these interactions, will be found in Reference [10].

I. EXPERIMENTAL

We have developed an experimental set-up designed to observe the motion of microscopic defects in a homeotropic slab of a SmA material submitted to a strain [9,10] (see Figure 1).

The cell is enclosed in a mK Instec oven under the microscope. A monolayer of surfactant (Cetylpyridinium Chloride) is coated on the glass plates of the cell in order to provide a strong hemeotropic anchoring of the liquid crystal molecules without disturbing the flatness of the substrate (we use optical quality glass floats). With such anchoring conditions in a wedge geometry (the angle α is fixed between 10^{-5} and 10^{-3} radians), a regular array of edge dislocations appears in the SmA phase of the sample [1]- the liquid crystal is a fluorinated octyloxyphenyl octyloxybenzoate that exhibits a SmC-SmA phase transition at T $\approx$ 54°C. Due to the variation of the local strain in the wedge, in the vicinity of the SmA-SmC transition, a temperature shift of this transition occurs along the dislocation. The local tilt of the molecules along the edge dislocations makes them visible in polarizing microscopy (see Figure 2).

The deformation of the cell (up to 0.2 μm) is controlled by a high voltage applied to a ceramic (typical deformation 2 Å·V^{-1}) and we record the associated motion of the dislocations with a CCD camera.

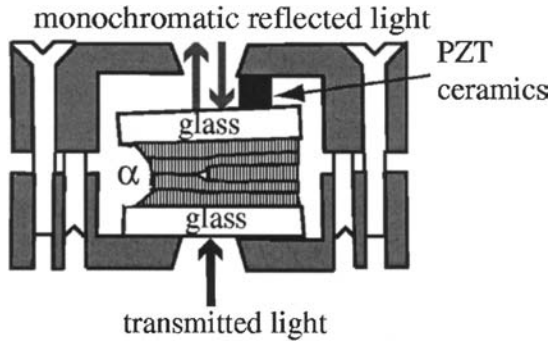

FIGURE 1 Deformation micro-device. The distance between the glass plates is tuned by the high voltage applied to the piezoelectric ceramic.

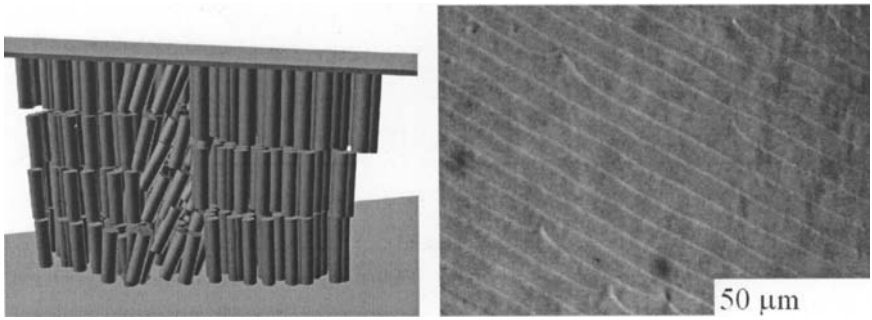

FIGURE 2 Due to a local shift of the SmA-SmC transition under strain (left), edge dislocations in the sample can be observed under polarizing microscope (view from above in the right picture).

II. RESULTS AND INTERPRETATIONS

1. Pinning of the Edge Dislocations at Rest

As shown on the right picture of Figure 2, edge dislocations are not always straight lines but are intermittently pinned on some fixed dots present in the samples. The shape of the edge dislocation is therefore made up of linear segments separated by cusps. These dots are not dust particles but rather the signature of screw dislocations. The latter originate at irregularities of one plate and cross the sample to the other plate, as evidenced by several observations [9–11] (see Figure 3). Note that we are able to tune the density of these screw dislocations by improving the cleaning of the plates [10].

In this note, we focus our interest to the shape of an edge dislocation pinned at the origin, first at rest in this section, then under motion (next section). We denote θ the local angle between the dislocation and the x-axis (see Figure 4). The presence of the Grandjean-Cano wedge angle α induces an elementary Peach and Koehler (PK) force [12] which acts on the dislocation line on any segment ds which is not at an equilibrium position Y_0 in the wedge. This force is given by:

$$d\mathbf{F_{PK}} = \frac{Bb\alpha(Y_0 - y)}{e} ds\mathbf{n} \tag{1}$$

where $\mathbf{n}$ is the unit vector normal to the dislocation, b the Burger vector of the dislocation of modulus $\delta \approx 35\,\text{Å}$ (the thickness of a smectic layer [11]), B the compression modulus of the layers and e the thickness of the cell.

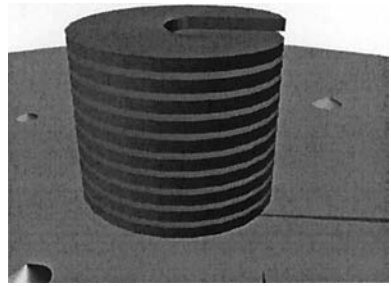

FIGURE 3 Sketch of a screw dislocation arising from irregularities present on the glass plate of a cell (a step in this sketch).

The PK force is opposed by a force due to the curvature of the dislocation:

$$d\mathbf{F}_{\mathrm{c}} = -\gamma \frac{d\theta}{ds} ds\mathbf{n} \tag{2}$$

where γ is the line tension of the dislocation, and $\mathbf{n}$ the unit vector normal to the dislocation. At equilibrium, the shape of the dislocation is obtained from the balance equation $d\mathbf{F_{PK}} + d\mathbf{F_c} = \mathbf{0}$. One gets:

$$1 - \cos\theta = \frac{Bb\alpha}{2e\gamma}(Y_0 - y)^2 \tag{3}$$

The force on the pinning dot, which results from the line tension is:

$$\mathbf{F}_{\gamma} = 2\gamma \sin\theta_0 \mathbf{y} \tag{4}$$

and opposes the force $\mathbf{F_p}$ due to the pinning of the dislocation at the origin.

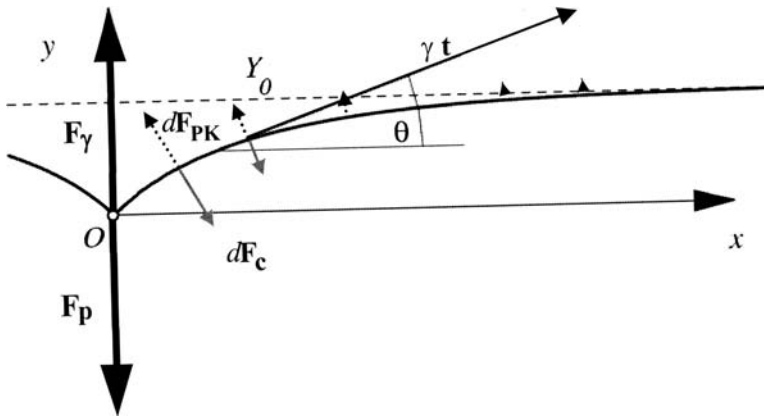

FIGURE 4 Forces acting on a pinned edge dislocation at rest (no external stress).

Note also that, using typical values (see Figure 2), $Y_0 = 10\,\mu m$, $\alpha = 5{\cdot}10^{-4}$ rad., $B = 10^6\,J{\cdot}m^{-3}$, $e = 10\,\mu m$, $\theta_0 \approx 45^\circ$, and $b = 3.5\,nm$ one can extract a value $\gamma \approx 10^{-12}\,N$ from Eq. (3), which is comparable to the value obtained in mixtures of 10CB and 8CB in Ref. [13].

2. Presence of a Yield Strain

When a strain is applied to a sample with very few pinning dots, we observe the *climb* (i.e. its movement in the plane of the dislocation array) of the edge dislocations under the corresponding PK force. We observe another situation for samples with a large density of screw dislocations: we clearly noted the existence of a yield strain below which the sample does not flow but behaves like an elastic medium (see Figure 5).

In samples with only a few screw dislocations (like in Figure 2), we observe that under strain, the length Y_0 increases as long as the dislocations are pinned, until they are suddenly released for a maximal distance $Y_{0,max}$.

Let $F_{p,max}$ be the maximal force supported by a screw dislocation. For small densities N_s of screw dislocations (individual pinning dots regime in Fig. 2), a pinned dislocation is submitted to a PK force, by unit length and far from the pinning point:

$$d\mathbf{F_{PK}} = bB\varepsilon\, dsy \tag{5}$$

where ε is the applied strain. On average, this force should be opposed to the total force due to the pinning dots. We thus obtain an order of the yield strain:

$$\varepsilon_0 \approx \frac{N_S F_{p,\max} Y_{0,\max}}{Bb} \tag{6}$$

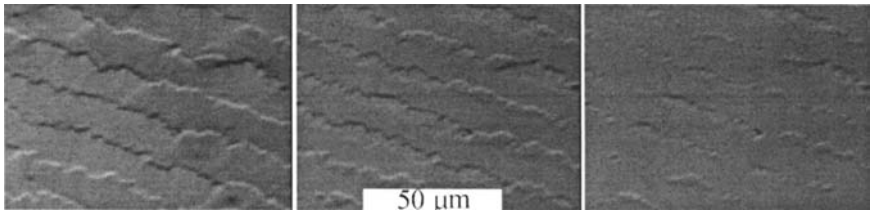

FIGURE 5 Motionless edge dislocations pinned by screw dislocations. From left to right, compressed, unconstrained, and dilated sample. The change of contrast is due to the corresponding local shifts of the SMA-SmC transition sketched in Figure 2.

3. Jerky-to-viscous Regime Transition

Above the yield strain ε_0, we enter in a plastic regime, *i.e.* the sample flows. Two different regimes [9] can be distinguished according to the strain-rate.

At low strain-rates, we observe a jerky motion of the edge dislocations characterized by the presence of pinning and unpinning processes. At each moment, the edge dislocations look like the dislocations of Figure 2, with several cusps. When the strain-rate increases we observe a progressive shortening of the unpinning distance $Y_{0,max}$ and the appearance (for a quite well defined strain rate) of a viscous regime in which the dislocations move as perfect strain lines in the cell. As an example, this transition occurs for a given strain-rate of $3{\cdot}10^{-4}\,\mathrm{s}^{-1}$ in the sample of Figure 2.

In order to explain such a transition, we consider now the forces acting on a moving edge dislocation (see Figure 6). Far from a pinning screw dislocation, a small length ds of an edge dislocation is submitted to a PK force.

$$d\mathbf{F_{PK}} = bB\varepsilon_l \, ds\mathbf{y} \tag{7}$$

where ε_l is the local strain that is different from the total applied strain because of the previous climb of dislocations within the wedge. This force is counted by a viscous force (see for example Ref. [14]).

$$d\mathbf{F_v} = -d\mathbf{F_{PK}} = -\frac{bv}{\mu}\, ds\mathbf{y} \tag{8}$$

where μ is the (free) mobility of the edge dislocations, and v their velocity.

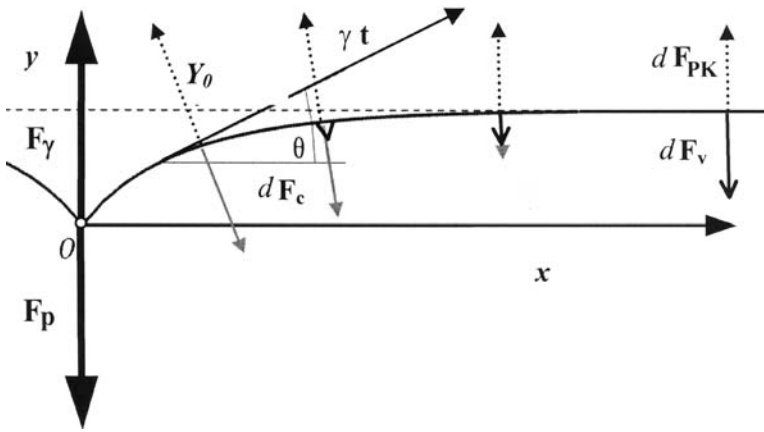

FIGURE 6 Forces acting on a climbing edge dislocation.

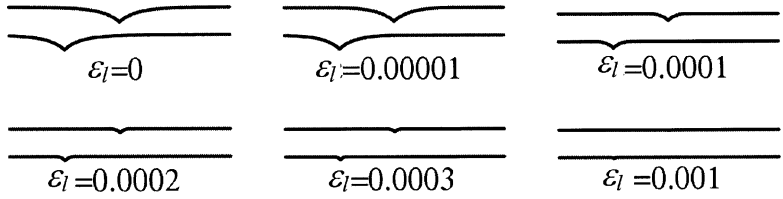

FIGURE 7 Evolution of the shape of pinned dislocation with the local strain.

This viscous force disappears in the pinned region (see Figure 6) but the PK force remains and is much larger than at rest. It varies now as:

$$d\mathbf{F_{PK}} = Bb\left(\frac{\alpha(Y_0 - y)}{e} + \varepsilon_l\right)ds\mathbf{n} \tag{9}$$

This force opposes to the curvature force defines the shape of the dislocation:

$$\begin{aligned} 1 - \cos\theta &= \frac{Bb\alpha}{2e\gamma}(Y_0 - y)^2 + \frac{Bb\varepsilon_l}{\gamma}(Y_0 - y) \\ &= \frac{(Y_0 - y)^2}{\Lambda^2} + \kappa\varepsilon_l\frac{(Y_0 - y)}{\Lambda} \end{aligned} \tag{10}$$

where $\Lambda = (2\gamma e/Bb\alpha)^{1/2}$ and $\kappa = 2e/\Lambda\alpha$.

If we consider now the distance of unpinning $Y_{0,max}(\varepsilon_l)$ for a moving dislocation that has been pinned by a screw dislocation, this latter is related to the distance of unpinning at rest $Y_{0,max,}$ according to:

$$Y_{0,max}^2 = Y_{0,max}^2(\varepsilon_l) + \kappa\varepsilon_l\Lambda Y_{0,max}(\varepsilon_l) \tag{11}$$

Figure 7 illustrates the evolution of the shape of a pinned dislocation with the local strain. The transition takes place within a small range of the local strain (which is linear with respect to strain rate).

The jerky-to-viscous transition is therefore not due to the disappearing of the pinning dots during the plastic flow but rather to the fact that the edge dislocations are stiffened by the PK forces due to the local strain.

4. CONCLUSION

The simple experiment we have designed yields important information on the actual mechanisms that control the plasticity of lamellar material. Our observations show in particular that the interactions of the screw dislocations present in a sample with the edge dislocations actually control the

flow mechanisms of an aligned smectic and should be carefully taken into account in the various mechanisms proposed for experiments in which lamellar phases are much more severely deformed.

REFERENCES

[1] Meyer, R. B., Stebler, B., & Lagerwall, S. T. (1978). *Phys. Rev. Lett.*, *41*, 1393.
[2] Bartolino & Durand, G. (1977). *Phys. Rev. Lett.*, *39*, 1346.
[3] Horn, R. G. & Kléman, M. (1978). *Ann. de Phys.*, *3*, 229.
[4] Bourdon, L., Kléman, M., Lejcek, L., & Taupin, D. (1981). *J. de Phys.*, *42*, 261.
[5] Oswald, P. & Kléman, M. (1984). *J. de Phys. Letters*, *45*, L319.
[6] Herke, R. A., Clark, N. A., & Handshy, M. (1995). *Science*, *267*, 651.
[7] Herke, R. A., Clark, N. A., & Handshy, M. (1997). *Phys. Rev. E*, *56*, 3028.
[8] Meyer, C., Asnacios, S., & Kleman, M. (2001). *Eur. Phys. J. E*, *6*, 245.
[9] Lelidis, I., Kleman, M., & Martin, J. L. (2000). *Mol. Cryst. Liq. Cryst.*, *351*, 187.
[10] Blanc, C., Zuodar, N., Lelidis, I., Martin, J.-L., & Kleman, M. (2004). *Phys. Rev. E*, *69*, no. 011705.
[11] Lelidis, I., Kleman, M., Martin, J. L., in preparation.
[12] Kleman, M. (1983). *Points, Lines and Walls: In Liquid Crystals, Magnetic Systems, and Various Ordered Media*, New York: John Wiley & Sons.
[13] Géminard, J. C., Holyst, R., & Oswald, P. (1997). *Phys. Rev. Lett.*, *78*, 1924.
[14] De Gennes, P.-G. & Prost, J. (1993). *Physics of Liquid Crystals*, Oxford: Clarendon Press.